LAWRENCE
LIVERMORE
NATIONAL
LABORATORY

UCRL-CONF-217023

MEMS Actuated Deformable Mirror

A. Papavasiliou, S. Olivier, T. Barbee, C. Walton, M. Cohn

November 11, 2005

SPIE MOEMS-MEMS 2006
San Jose, CA, United States
January 21, 2006 through January 27, 2006

MEMS Actuated Deformable Mirror

Alexandros Papavasiliou[a], Scot Olivier[a], Troy Barbee[a], Chris Walton[a], Michael Cohn[b]
[a]Lawrence Livermore National Laboratory, 7000 East Ave. Livermore CA 94550
[b]MicroAssembly Technologies, 3065 Richmond Parkway Suite 109, Richmond CA 94806

ABSTRACT

This ongoing work concerns the creation of a deformable mirror by the integration of MEMS actuators with Nanolaminate foils through metal compression boning. These mirrors will use the advantages of these disparate technologies to achieve dense actuation of a high-quality, continuous mirror surface. They will enable advanced adaptive optics systems in large terrestrial telescopes.

While MEMS actuators provide very dense actuation with high precision they can not provide large forces typically necessary to deform conventional mirror surfaces. Nanolaminate foils can be fabricated with very high surface quality while their extraordinary mechanical properties enable very thin, flexible foils to survive the rigors of fabrication. Precise metal compression bonding allows the attachment of the fragile MEMS actuators to the thin nanolaminate foils without creating distortions at the bond sites.

This paper will describe work in four major areas: 1) modeling and design, 2) bonding development, 3) nanolaminate foil development, 4) producing a prototype. A first-principles analytical model was created and used to determine the design parameters. A method of bonding was determined that is both strong, and minimizes the localized deformation or print through. Work has also been done to produce nanolaminate foils that are sufficiently thin, flexible and flat to be deformed by the MEMS actuators. Finally a prototype was produced by bonding thin, flexible nanolaminate foils to commercially available MEMS actuators.

Keywords: MEMS, Deformable mirrors, Nanolaminates

1. INTRODUCTION

This work is aimed at fulfilling the need for a moderately sized deformable mirror with thousands of pixels for adaptive optics for large terrestrial telescopes. We will combine the excellent material properties and optical quality that can be achieved with nanolaminate foils with the high density actuation possible with MEMS actuators.

1.1. Goals and Specifications

The purpose of this project is to demonstrate a technology to produce deformable mirrors that have a low-spatial-frequency stroke of 5-10μm, a high-spatial-frequency deflection of 1-3 μm, a pixel spacing of around 1mm and scalable to arrays with on the order of 1000 pixels.

1.2. BMC MEMS actuators

Boston Micromachines Corporation produces the most mature MEMS SLM available[1]. Their devices can produce deflections on the order of 5μm on a pitch of 400μm. Unlike many other technologies, large arrays produced by BMC have been shown to work with fairly high yield. While they don't generate very much force, these arrays provide the necessary actuator density. When mated with thin, flexible nanolaminate mirror surfaces, they should produce a continuous deformable mirror with dense actuation.

The BMC devices consist of three layers, A stiff silicon base with electrodes and wires patterned on it, a polycrystalline silicon actuator layer that is held above the base with stiff silicon posts called vias, and a mirror that is supended above the actuator with a via. The actuator and mirror are electrically grounded. When a voltage is placed on the electrode on the base, the actuator is drawn towards the base by electrostatic force. The mirror, which is rigidly attached to the moving actuator layer moves producing the desired deformation.

1.3. Nanolaminates

Nanolaminates are thin, flexible, optically smooth metal foils with very high strength. The ability to make an optically smooth foil that is both tough enough to withstand fabrication and thin enough to be very flexible makes a good match with the high density but low force provided by MEMS actuators.
A nanolaminate foil is a metal foil created by sputtering thin layers of metal one on top of the other. The foils are deposited on a mandrel with a release layer that allows them to be parted from the mandrel. With a sufficiently thin and conformal release layer, the foils take on the shape of the mandrel, and an optically smooth mandrel yields an optically smooth foil. The layers are deposited by magnetron sputtering over a moving table. The thickness of each individual layer as well as the whole thickness of the foil can be accurately controlled. By varying the rotation speed of the table individual layers can be made with thicknesses from 10Å to 1mm. The very thin layers prevent growth of large grains stopping dislocation motion and strengthening the material in the same way precipitates strengthen steels. The resulting layered composite has an ultimate tensile strength 2-3 times that of either constituent. This high strength allows one to fabricate foils that are both thin enough to allow them to be deformed by very weak MEMS actuators and still strong enough to be handled and bonded to the MEMS actuators.

1.4. Bonding

The third technology necessary for MEMS-actuated nanolaminate deformable mirrors is bonding. The metal foils must be bonded to the MEMS actuators with sufficient strength to hold together and the bonding process must not destroy the MEMS actuators. MicroAssembly Technologies is a pioneer in the field of bonding to MEMS structures through metal compression bonding[2]. Both metal compression bonding[3] and adhesive bonding have been used in the work presented here.

2. MODELING AND DESIGN

The system was modeled in order to determine the design parameters that will allow this system to reach the specified performance. Since the actuators used in this project are off-the-shelf devices, all of their parameters have already been set. The mirror parameters have not been previously set, however, there is some lower limit on how thin and flexible the mirror can be while still withstanding the rigors of fabrication. The real goal of the modeling, then was to determine the thickest foil that would yield meaningful high-spatial-frequency deformations.
The modeling was broken up into the two major components of the device, the actuator and the nanolaminate mirror. While the BMC actuators to be used in this system are in existence and can be measured, they must be understood enough to determine how they will interact with a nanolaminate mirror. The mirror itself must be modeled to determine how much it will resist deformation into high spatial frequency shapes. Finally the two pieces are combined into a complete system.

2.1. Actuator

The BMC actuator is a “double cantilever” design. This means that it consists of a flat plate that is built-in at both ends and suspended above an electrode. The plate has four large cutouts that decrease its stiffness. The electrode on the base of the actuator is split into two pieces, to decrease the electrostatic force and increase the stable range of operation.
The actuator deforms to move down, towards the electrode. For this model, we modeled the deformation along the width of the actuator assuming that the deformation is uniform though the depth of the actuator. The electrostatic attraction is a function of the gap between the electrode and the actuator layer, thus it varies with deflection and with position along the width of the actuator.
The governing equation for the deformation of a plate including both bending and stretching can be written as:

$$\nabla^4 z = \tfrac{1}{D}\left(q(x) + \tfrac{1}{2}\frac{Et}{\left(1-\nu^2\right)}\left(\left(\tfrac{\partial z}{\partial x}\right)^2 \tfrac{\partial^2 z}{\partial x^2}\right)\right) \qquad [1]$$

Where Z is deflection, Q is the load, D is a measure of the stiffness of a unit area of the plate, E is young’s modulus, t is thickness, and ν is Poisson’s ratio. The load is a combination of the point load of the post in the center of the actuator and the electrostatic load. The electrostatic load is

$$q(x) = \tfrac{1}{2}\frac{\varepsilon_o w V^2}{(g-z)^2} \qquad [2]$$

Plugging the load equation into the governing equation, and assuming that neither load nor deformation vary with depth (y-direction) of the actuator, the system is an ordinary differential equation where the fourth derivative of position is a function of the second derivative and of position itself. Such a system is easily solved with a numerical differential equation solver.

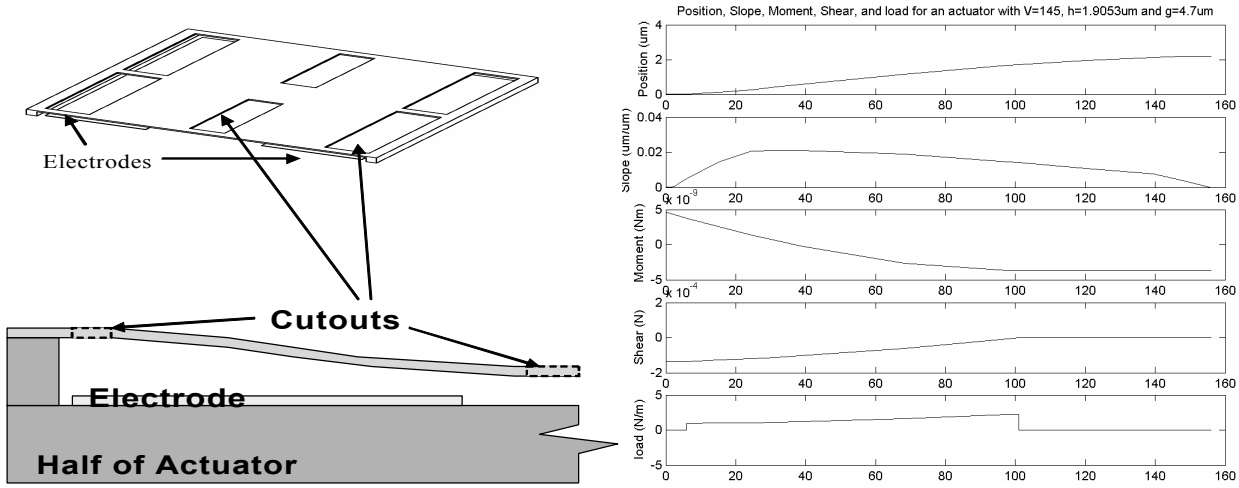

Figure 1: Drawing of actuator, schematic of simulated portion of actuator, and typical results of actuator simulation showing load, shear, moment, slope and deformation.

The results of a numerical model for the deformation of a BMC MEMS actuator is shown above. Since the deformation is symmetric, only half of the device is calculated. Note that there are two steps in the load curve indicating each end of the electrode. The load slopes upward as the deformation increases towards the center of the actuator. Shear, the integral of load, shows that the slope of the shear is non-zero where there is load, above the electrode. Moment is the negative integral of shear. The slope of the actuator begins and ends at zero, as would be expected for a built in end, and the midpoint of a symmetric plate. The slope plot also exhibits distinct changes in slope at the positions of the cutouts.

2.1.1. Comparison with BMC data

BMC provided us with some experimental data on the deflection of the MEMS actuators as a function of voltage. Their experimental data showed that the MEMS actuator reached a deflection of 2.2μm at a voltage of 145V. The nominal gap and thickness of the device were 4.7μm and 2μm. We found that our model correlated best with the data when the gap was set to 4.7μ and the actuator layer thickness was set to 1.905μm.

2.2. Mirror Modeling

The next important portion of the model is the mirror. The mirror in this case will be a continuous nanolaminate foil attached by posts to the MEMS actuators. In order to design a system that will achieve high-spatial-frequency shapes, we need to model how the mirror resists bending into those shapes. The governing equation of the deformation of the mirror can be written as:

$$\nabla^4 z = \frac{1}{D}\left(q + \frac{1}{2}\frac{Eh}{\left(1-\nu^2\right)}\left(\left(\frac{\partial z}{\partial x}\right)^2 \frac{\partial^2 z}{\partial x^2}\right) + \left(\left(\frac{\partial z}{\partial y}\right)^2 \frac{\partial^2 z}{\partial y^2}\right)\right) \qquad [3]$$

Unlike the actuator plate which could be simplified to a plate with deformations that only vary with one horizontal direction, the mirror definitely deforms with respect to both X and Y. Thus the solution for the problem is a partial differential equation instead of an ordinary differential equation. Numerically solving a PDE is much more challenging than an ODE. We solved this problem by simplifying it to a repeating high-spatial-frequency pattern for which a solution could be found.

2.2.1. Checkerboard pattern

We chose to model the mirror with a "checker board" actuation pattern where every other actuator is pulled down with the maximum potential and the alternate actuators are not actuated. The checkerboard is a repeating high-spatial-frequency shape that can be easily modeled. It can be seen from inspection that each element in a checkerboard loaded plate is a square plate with a point load in the center and simply supported at each edge.

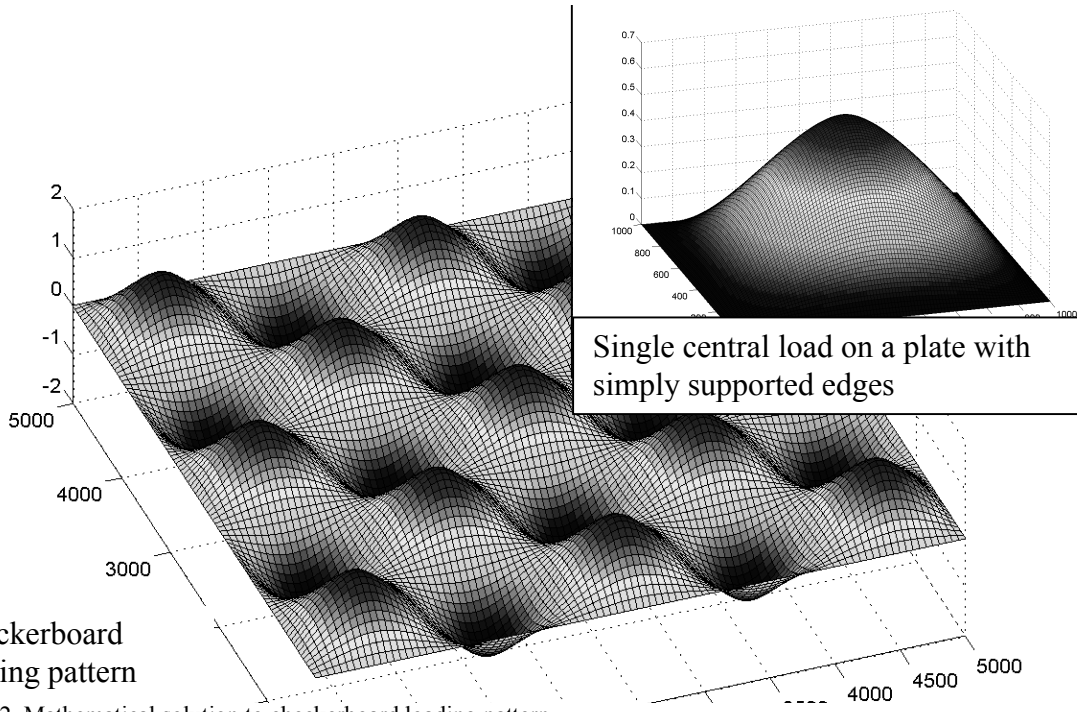

Figure2. Mathematical solution to checkerboard loading pattern

2.2.2. Plate Simulation

We found the shape of the deformation by solving for the simpler case of small deflections, where the resistance of the plate to stretching is considered negligible. The small deflection approximation is a good assumption when the deflections are smaller than the thickness of the plate. In this case, the deflections are on the order of the thickness of the plate and resistance to stretching should be considered. However, it is generally accepted that a good approximation to the true resistance to deformation can be found by using the small deflection approximation to find the shape, then finding the restoring force by calculating the strain energy of the small deflection shape[4]. In this case, the governing equation for the small deflections is:

$$\nabla^4 z = \frac{q}{D} \qquad [4]$$

If the loads are written as the sum of a series of sine functions, the deformation will be the fourth integral of those loads, and thus a series of the same sine functions. Thus for a rectangular plate Navier's solution to this problem is to create a geometric series[4]:

$$z(x,y) = \frac{1}{\pi^4 D}\sum_{m=1}^{\infty}\sum_{n=1}^{\infty}\frac{a_{mn}}{\left(\frac{m^2}{l_x^2}+\frac{n^2}{l_y^2}\right)^2}\sin\left(\frac{m\pi x}{l_x}\right)\sin\left(\frac{n\pi y}{l_y}\right) \qquad [5]$$

where a is a matrix of constants determined by the loading conditions such that the load is

$$q(x,y) = \sum_{m=1}^{\infty}\sum_{n=1}^{\infty}a_{mn}\sin\left(\frac{m\pi x}{l_x}\right)\sin\left(\frac{n\pi y}{l_y}\right) \qquad [6]$$

Note that the edges of this solution will always have a position of zero, a finite slope, zero curvature corresponding to zero moment, a finite third derivative corresponding to a finite shear, and a zero fourth derivative corresponding to zero load. So, the solution accurately describes a simply supported edge.
For a point load at the center of a rectangular plate, the matrix a can be found to be:

$$a_{mn} = \frac{4F}{l_x l_y}\sin\left(\tfrac{m\pi}{2}\right)\sin\left(\tfrac{n\pi}{2}\right) \qquad [7]$$

The deflection at any point on the plate can now easily be found as a function of plate geometry and the magnitude of a central point load P.
To find the large-deflection restoring force, we use the large deflection equations for strain energy:
The energy from bending is

$$dU_{bending} = \tfrac{1}{2} D\left\{\left(\tfrac{\partial^2 z}{\partial x^2} + \tfrac{\partial^2 z}{\partial y^2}\right)^2 - 2(1-\nu)\left[\tfrac{\partial^2 z}{\partial x^2}\tfrac{\partial^2 z}{\partial y^2} - \left(\tfrac{\partial^2 z}{\partial x \partial y}\right)^2\right]\right\} dx\, dy \qquad [8]$$

The energy from stretching is:

$$dU_{stretching} = \frac{Et}{8(1-\nu^2)}\left[\left(\tfrac{\partial z}{\partial x}\right)^4 + \left(\tfrac{\partial z}{\partial y}\right)^4 + 2\nu\left(\tfrac{\partial z}{\partial x}\right)^2\left(\tfrac{\partial z}{\partial y}\right)^2\right] dx\, dy \qquad [9]$$

From this we can find the strain energy and the restoring force as functions of displacement. We wrote a MATLAB script to calculate the matrix of coefficients for a unit point load and, from that, the shape of the deformed plate. A second MATLAB script calculated the energy as a function of the shape. We performed this calculation for plates with a variety of plate parameters and simplified the equations for energy and force to:

$F = K_1 Z + K_3 Z^3$ where

$$K_1 = 86.37\frac{D}{L^2}, and \quad K_3 = \frac{Et}{L^2}\left(7.996 + 1.401\nu + 5.443\nu^2 + 10.35\nu^3\right) \qquad [10]$$

This relation only describes the deformation of one square element, in the checkerboard deformation pattern each neighboring square has an equal and opposite deformation. The deformation described above is only half of the total pixel-pixel deformation. The coefficients with respect to the pixel to pixel deformation are ½ and 1/8 of the above coefficients.

$$K_1 = 43.19\frac{D}{L^2}, and \quad K_3 = \frac{Et}{L^2}\left(0.9995 + 0.1751\nu + 0.6804\nu^2 + 2.588\nu^3\right) \qquad [11]$$

2.3. Integrated system

With models for the two major components of the deformable mirror, the next problem is to combine the two to find the high-spatial-frequency response of the entire system. One of the advantages of the checkerboard pattern is that there are an equal number of actuated and un-actuated pixels. Thus the force applied by each actuated pixel on the mirror must equal the force applied by the mirror on each un-actuated pixel.

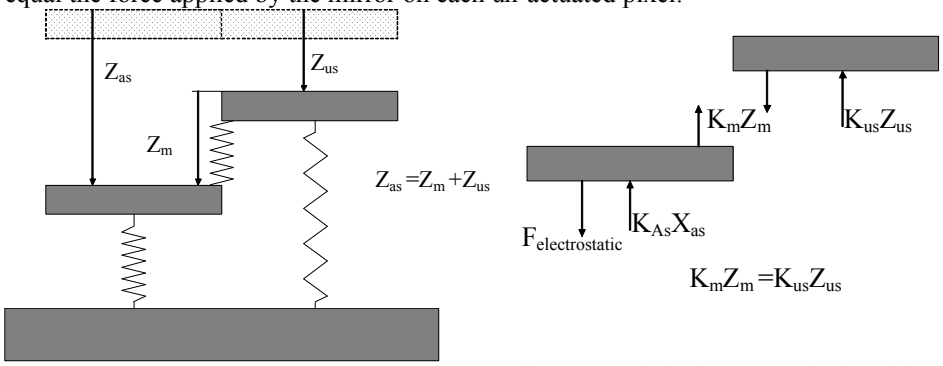

Figure3.On the left is the schematic of the actuated/un-actuated pixel system. The dotted boxes indicate the rest position of both pixels, the grey boxes indicate the deformed position of the pixels. The pixel on the left is pulled down electrostaically, the pixel on the right is pulled down by the mirror. The mirror is represented by a sprig between the two pixles. On the right is the free-body diagram of the two pixels.

As shown in the diagram above, the deflection of the actuated pixel, Z_{as} must be equal to the sum of the deflection of the mirror Z_m and the un-actuated pixel Z_{us}. From the free-body diagram of the two pixels, the force translated through the mirror must be equal to the restoring force of the deformed mirror and the restoring force of the un-actuated pixel. From the actuator model, we can find the electrostatic force as a function of displacement. This gives us 3 equations and 3 unknowns, so we can solve for the displacement of all three portions of the system.

2.4. Design based on the analytical model.

Since the MEMS actuators have already been designed and fabricated, the only parameter that can really be adjusted for this device is the foil thickness. The foil must be simultaneously thin enough to be deformed and thick enough to be readily handleable. With the model described above, we found the ratio of high-spatial-frequency displacement to low-spatial-frequency displacement as a function of mirror thickness. As shown in the plot below, the ratio decreases as the foil thickness increases. We felt that 5µm was around the limit of how thin a foil could be and still be handleable. The plot below shows that the ratio at 5µm is around 7.8%. We believe that a ratio on the order of 10% is sufficient for a demonstration, so we chose 5µm as the foil thickness.

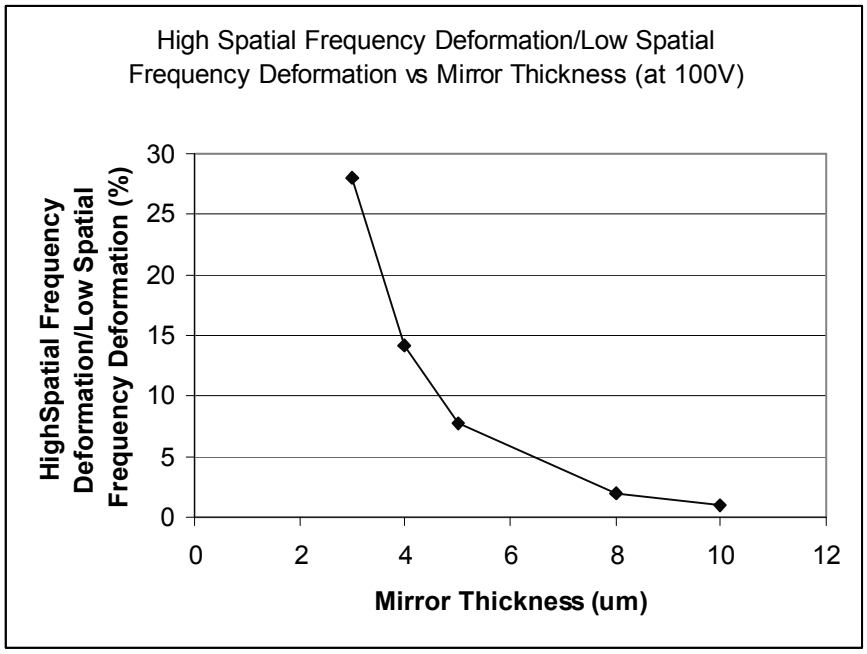

Figure 4. Ratio of high-spatial-frequency deformation to low-spatial-frequency deformation as a function of mirror thickness.

The ratio is actually better than is shown in the plot above. Although the model shows a single actuator snaps down at 2.32µm and 146 Volts, the high-spatial frequency checkerboard shape can be driven at higher voltages and achieve 244nm displacement at 179 Volts. Thus the high-spatial-frequency displacement 10.5% of the low-spatial-frequency displacement.

3. NANOLAMINATE DEVELOPMENT

3.1. Producing the foils

The nanolaminates for this project were produced in a magnetron sputtering machine at LLNL. The chamber contains 4 magnetron sputter sources: two are 5" X 10", for the main two materials, copper and zirconium, and two are 4" circular for thin gold under and over layers, and release layer. The 6 inch silicon wafers used as mandrels are mounted on a table that both rotates them about their axis and revolves them around the axis of the chamber.

Before sputtering the foils, the chamber is pumped down to $5X10^{-8}$Torr. A thin release layer is sputtered on the substrates. Next, a thin gold termination layer is deposited. The bulk of the nanolaminate foil is produced by running

both copper and zirconium targets simultaneously while revolving the mandrels past the targets. The system is operated for a given number of revolutions to achieve the specified thickness (5-50nm). Finally a gold layer is deposited terminating the top of the foil.
When the foil is ready to be parted from the mandrel it is parted with a razor blade and tweezers.

3.2. Foil Post Processing

After the foils are produced, metal bumps must be deposited and the foils must be diced into appropriately sized pieces. While still attached to the silicon mandrel, metal bumps are electroplated through a photoresist mask onto the nanolaminate foil. The photoresist mask is removed and another mask is patterned to define the dicing lines. The foils are diced by chemical etching. A potassium iodide solution is used to etch the gold layers, and a mixture of buffered hydrofluoric acid and nitric acid is used to etch the copper zirconium foil.

3.3. Foil Curling

Foil curling is an enormous problem in nanolaminate deformable mirrors. Large amounts of curling make it difficult to handle the foil during the bonding process. More moderate amounts of curling can cause the fragile MEMS actuators to break. Even seemingly small amounts of curling can overwhelm the dynamic range of the MEMS actuators.

3.4. Curling sources

While the work done for this project has succeeded in greatly reducing the amount of curl present in the foils used for this project, the problem is not completely understood. We have, however been able to identify a possible dominant effect, and some hypotheses on secondary effects.

3.4.1. Heating during deposition

Although further work will need to be performed to fully understand the cause of curling, we believe the dominant effect comes from the heating of the mandrel during the deposition process. The first layers of the foil are deposited at room temperature. As subsequent layers are deposited, the mandrel is heated by the plasma and expands. Since the foil has a greater CTE than the mandrel, the first layers of the foil develop a compressive stress in addition to the stress they had at deposition. The top layers of the foil are deposited on top of the hot expanded mandrel. Both the mandrel and foil shrink as they return to room temperature. Since the foil has a higher CTE than the mandrel, the top layers are stretched while the bottom layers are returned to their deposition stress. When the foil is parted from the mandrel the stress differential causes the foil to curl.

3.4.2. Additional Effects

3.4.2.1. Deposition stress variation with temperature

The stress at which a film forms is highly dependent on the temperature of the substrate on which it is deposited. The difference between the deposition stresses of the top and bottom of the foil may be greater than the thermally generated stress. However, the deposition stress is not well characterized as a function of temperature.

3.4.2.2. Release effects

The curling in these foils is generally great enough to force the foil into a cylindrical shape. We have observed that the orientation of the axis of the cylinder is well correlated to the direction of release. Even when forced flat or into a cylindrical shape with a different orientation, the axis of the cylinder returns to the original shape. This observation strongly suggests an effect that occurs during the release

One hypothesis for the cause of the release-related curling is that a stress concentration at the interface between attached and released foil causes local plastic deformation. The localized plastic deformation results in stress the causes curling.

A second hypothesis for the cause of the release related curling is permanent deformation from the bending during the release. The foil is released with a razor blade and tweezers. There is generally an upward force exerted by the tools which causes bending in the foil. This bending can cause a permanent deformation about two orders of magnitude less than the initial bending. While it is hard to believe that this effect could cause all the curling we observe, it is possible that in the absence of any other directional preference it produces enough stress to orient the foil.

3.5. Curling minimization

The curling of the nanolaminate foils was eliminated by pre-heating the mandrels in order to keep the mandrel at a constant temperature during deposition. The mandrel was pre-heated with a quartz lamp placed in the chamber. The temperature of the mandrel was measured with thermocouples and a heating recipe was developed that maintained a fairly constant temperature during the deposition.

4. BONDING

Two types of bonding have been experimented with for these devices. 1) metal compression bonding where a metal bump is deformed against a metal pad making an electrical and mechanical connection. 2) epoxy bonding where a 2-component epoxy is compressed between the metal pieces and cured. Preliminary experiments were performed by bonding nanolaminate foils to dummy chips. Later work has been performed to try to bond the nanolaminate foils to MEMS actuators.

4.1. Print-through minimization with dummy chips

One of the major concerns in this project was that the bond should not create a large deformation in the mirror surface of the nanolaminate foil. The first experiments were performed to find the magnitude of the print-through problem and to find ways to eliminate it. This experiment was performed by electroplating gold bumps onto a dummy chip then pressing the nanolaminate foil against the dummy deforming the bumps to create bonds.

4.1.1. First Experiment

The first experiments showed surface features on the order of 1.5µm both around the bond site and elsewhere. These features suggested an intermetallic may have been forming between the gold termination layer and the steel chuck.

4.1.2. Inermetallic elimination

The intermetallic was eliminated by switching to a silicon nitride coated chuck. In addition, the bonding material was switched from gold to a MAT proprietary gold indium The next experiments yielded samples that while smoother, indicating no intermetallic bonding, still had deformations on the order of 2µm.

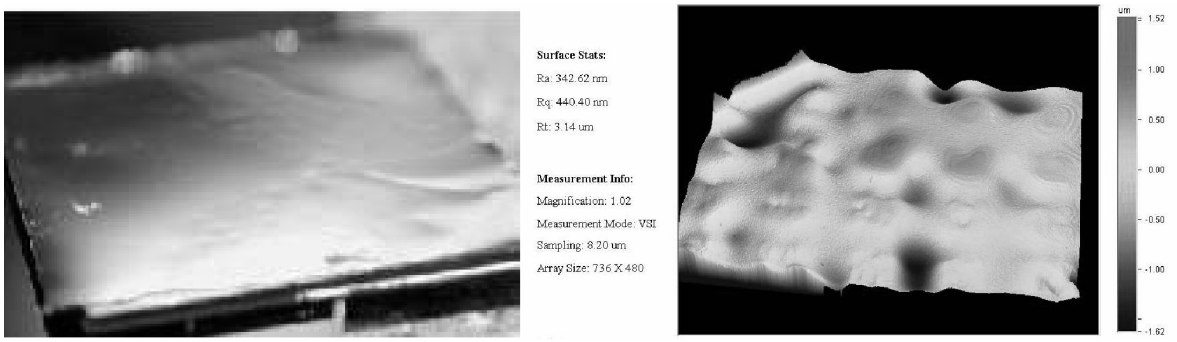

Figure 5. Optical photograph of foil as well as surface map.

4.1.3. Parameter optimization

The system was modeled with finite element software allowing MicroAssembly Technologies engineers to optimize the bonding parameters. The metal bond material was changed to a proprietary gold-indium mixture allowing a lower temperature bond. These improvements produced a bonded foil with deformations on the order of 25nm peak to peak which, do not correspond to the location of the bonding posts.

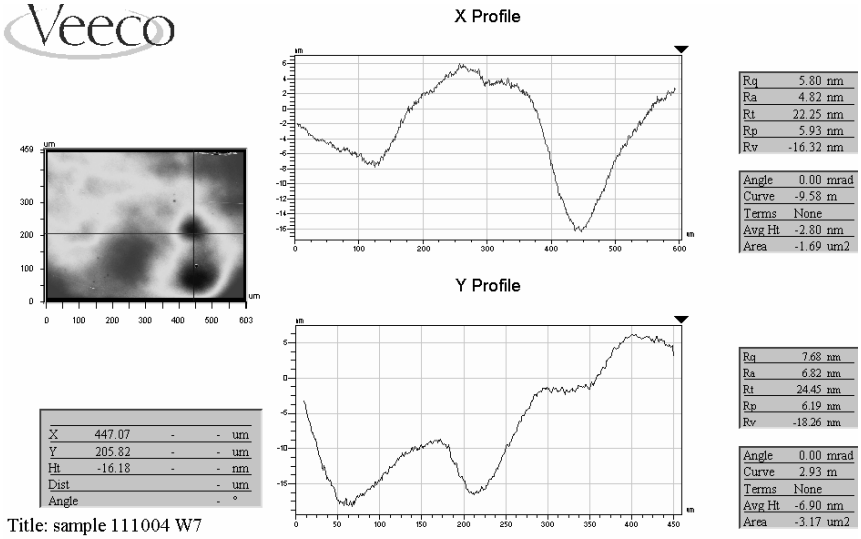

Figure 6. surface map of optimally bonded foil. Note peak to peak deformation <25nm.

4.2. The MEMS actuator bonding experiment

The first bonding attempt of a nanolaminate foil to an array of MEMS actuators was a failure. The foil used for this experiment was not completely flat. After the bond, as the foil chuck pressure was removed, the foil curled away from the MEMS actuator chip. Upon investigation, the bond appears to be successful, however, the polysilicon MEMS parts broke. Future bonding experiments will be done with flat foils.

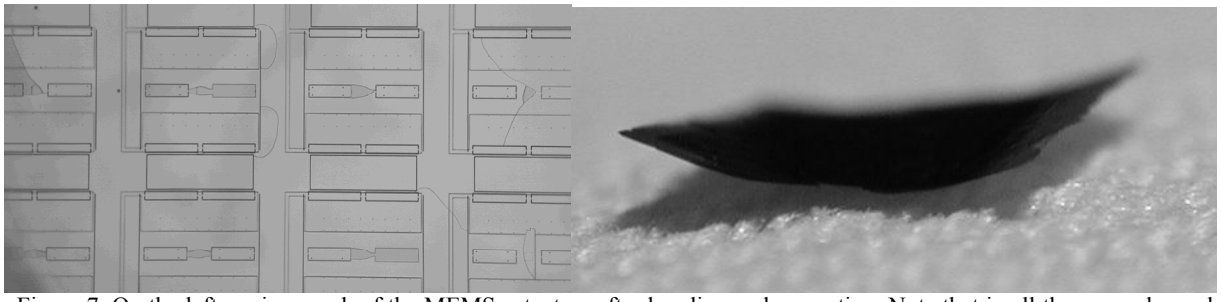

Figure 7. On the left a micrograph of the MEMS actuators after bonding and separation. Note that in all the cases shown here, the silicon MEMS actuator has broken indicating a sufficiently strong bond. On the right a photograph of the separated nanolaminate foil after bonding.

5. CONCLUSION

This paper presents a technology to fabricate deformable mirrors based on a combination of MEMS actuators and nanolaminate foils. The devices were modeled and the system was designed based on those models. Although working prototypes have not been produced yet, considerable work has been done to enable these devices. Bonding techniques have been developed that minimize the print-through to the mirror surface. The problem of curling of metal foils has been largely solved by controlling the temperature of the mandrel during deposition.

ACKNOWLEDGEMENTS

This work was performed under the auspices of the U.S. Department of Energy by University of California, Lawrence Livermore National Laboratory under Contract W-7405-Eng-48.

REFERENCES

1. Zhu, H., Bierden, P. A., Cornelissen, S., Bifano, T.G., Kim, J.H., "Design and fabrication of reflective spatial light modulator for high-dynamic-range wavefront control,"Proc. SPIE Vol. 5553, Advanced Wavefront Control: Methods, Devices, and Applications II, Oct 2004.
2. Singh, A.; Horsley, D.A.; Cohn, M.B.; Pisano, A.P.; Howe, R.T.; "Batch transfer of microstructures using flip-chip solder bonding," *Microelectromechanical Systems, Journal of* Volume 8, Issue 1, March 1999 Page(s):27 – 33
3. Humpston, G., and Baker, S.J. "Diffusion Bonding of Gold, " *Gold Bulletin*, 1998, 31 (4)
4. Timoshenko, S. and Woinowsky-Krieger, S.; *Theory of Plates and Shells*, McGraw-Hill, NewYork, 1959